Journal of Ocean, Mechanical and Aerospace
-Science and Engineering-, Vol.38

December 30, 2016

Prediction of Flow Distribution in Cooled Gas Turbine Blade with Ribs, Pin-Fins and Film Cooling Holes in Leading Edge Passage

Dr. Sachin L. Borse

[a)] *Professor, Mechanical Engineering, J. S. P. M's Rajarshi Shahu College Of Engineering, Savitribai Phule Pune University, Pune, India*

*Corresponding author: *sachinlb@yahoo.co.uk*

Paper History

Received: 14-September-2016
Received in revised form: 20-December-2016
Accepted: 30-December-2016

ABSTRACT

Modern gas turbine blade is internally cooled to maintain its temperature at safe level. Prediction of mass flow distribution in cooling passage of the turbine blade helps in predicting turbine blade temperature during the design stage. In this current paper, commercial software FLUENT 6.2 is used to predict mass flow distribution in the gas turbine blade cooling passages (like leading edge passage, serpentine passage, trailing edge passage, lateral ejection, tip and film cooling holes) with standard k-ε and RNG k-ε turbulence models. Model suitable to solve such problem requires huge computational resources. Although present model are not suitable for the problem considered but will help to get approximate results and will also indicate capability of CFD. Results are compared with experimental results. Result showed good agreement of predicted mass flow distribution with experimental results. RNG k-ε model shows slight improvement in prediction of the supply pressure over other two models.

KEY WORDS: *Gas turbine blade cooling, CFD, flow distribution*.

NOMENCLATURE

d	Hydraulic diameter of passage
d_A	Diameter of tip hole
d_B	Diameter of serpentine passage end hole
d_h	Hydraulic diameter of passage
d_{imp}	Diameter of leading edge impingement hole
e	Height of rib
k	Turbulent kinetic energy
p	Pressure
pin	Inlet pressure
$pexit$	Pressure in header in each passage
P	Pitch of rib
rd	dB/dh
Re	Reynolds number based on hydraulic diameter
$\dot{m}$	Mass flow rate
$\dot{m}_{LL}$	Mass flow rate-leading leading most passage
$\dot{m}_{LS}$	
$\dot{m}_{SE}$	Mass flow rate-leading supply passage
$\dot{m}_{ST}$	Mass flow rate –serpentine passage end hole
$\dot{m}_{TT}$	
$\dot{m}_{TL}$	Mass flow rate-serpentine tip Mass flow rate-trailing edge passage tip Mass flow rate-trailing edge passage lateral ejection
$\dot{m}_{FL}$	Mass flow rate-leading edge passage film cooling
$\dot{m}_{tot}$	Total mass flow rate
$\%\dot{m}_{tot}$	Percentage of total mass flow going to given stream
$\%\Delta\dot{m}$	Percentage difference in prediction of mass flow rate
$\%\Delta p$	Percentage difference in predicted and measured supply pressure taking measured pressure as reference.

1.0 INTRODUCTION

Modern gas turbine blades are cooled internally and externally to ensure longer life of the turbine blade. Figure 1 shows a typical cooled turbine blade. Cross section of the blade consists of three distinct passages viz., a) Leading edge coolant passage, having holes for impingement cooling, b) middle serpentine passage with turbulence promoters like ribs and c) Trailing edge passage with pin fins and lateral ejection holes. Leading edge passage is always provided with film cooling holes. In some cooled blades,

serpentine and trailing edge passages also have film cooling holes. Film cooling holes are provided to protect the blade thermally by extracting heat as coolant passes through holes and by forming a protective layer of relatively cold air on external surface. Optimum design of the cooling system requires knowledge of external heat load to the blade and heat transfer coefficient distribution in internal passages. With this information, temperature distribution in the blade can be estimated. The passage heat transfer coefficient, in turn, depends on mass flowing through the passage.

Experimental studies on flow distribution in gas turbine blade are reported by Borse and Date [2,3]. Numerical study on flow distribution without pin-fins, ribs and film cooling holes is reported by Borse [4] and numerical study on flow distribution with pin-fins and, without ribs and film cooling holes is reported by Borse [5]. Numerical study with ribs and pin-fins is reported by Borse [6]. This current paper takes into account presence of film cooling holes in leading edge passage with ribs and pin-fins in serpentine and trailing edge passages respectively. To the best of author's knowledge, no such numerical study on flow distribution with film cooling holes is reported in the open literature.

Design of cooled gas turbine the blade changes from one manufacturer to the other. Information on exact dimensions of a modern cooled turbine is scanty. The available information from the literature is shown in Table 1. Han et al. [1] give dimensions of blade tip holes. This information clearly indicates that the tip hole at the end of the serpentine passage is bigger than other tip holes. The tip holes are meant for cooling the tip area of the blade. Compared to the leading- and the trailing edge passages, the serpentine passage with two 180^{o} bends is most tortuous and therefore it is necessary to have relative bigger tip-hole for this passage to achieve reasonable flow rate through this passage.

Several turbulence numerical models are used to predict fluid flow and heat transfer in gas turbine blade. Han et al [1] describes numerical modeling related to turbine blade cooling. For internal fluid flow and heat transfer generally k-ε, k-ω and their variants, and RSM (Reynolds Stresses Modeling) are used. Also LES and DNS approach are used to study effects of turbulators on pressure drop and heat transfer in ribbed passage.

Suitable models, RSM and low Re k-ω or low Re k-ε models requires huge computation efforts. In this current study, standard k-ε, and RNG k-ε models are used with wall function, which do not demand huge computation resources. These current models will not map all secondary flows and anisotropy in turbulence but will help to get approximate estimates of flow distribution and supply pressure.

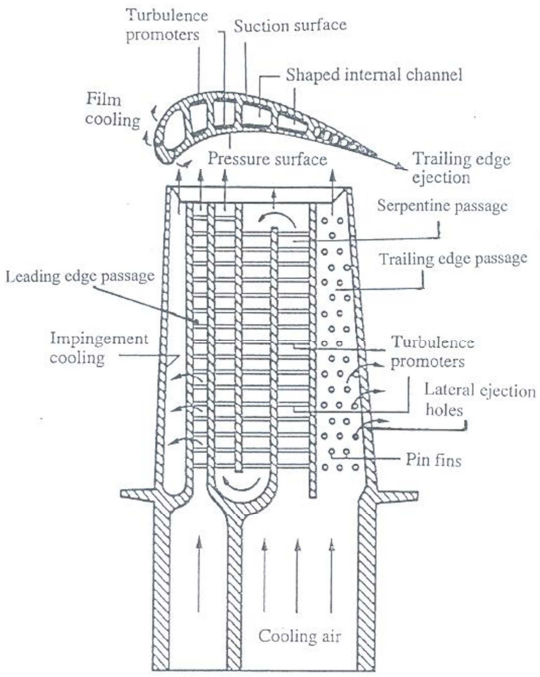

Figure 1: Schematic of a Modern Cooled Gas Turbine Blade [1]

Table 1: Typical aircraft turbine blade cooling parameters for serpentine passage (Hwang et al [7])

Parameters	Values
Coolant passage hydraulic diameter, mm	~4
Coolant passage length, mm	48-70
Rib height to diameter of passage ratio, e/dh	0.01-0.15
Pitch to height ratio of ribs, P/e	7-13
Mean coolant velocity (m/s)	34.5-69
Flow Reynolds number, Re	20,000-40,000

2.0 EXPERIMENTAL SET-UP

Figure 2 shows details of the experimental set-up. The test section is a scaled up (approximate 5 times) simplified cold model of the turbine blade. Air to the test section is supplied from 10 hp blower through a flow control valve, a diffuser and a settling chamber. The test section, whose internal cross section area is much smaller than that of the settling chamber is fed directly from the settling chamber to simulate sudden contraction condition prevailing in the plenum of the gas turbine blade. Unlike the real blade, the test section is symmetric. It is made in split form, from two Perspex slabs (see Figure 3). On these slabs, passages are milled in such way that half portion of the passage lies in lower slab and the other half in the upper slab. These two slabs are bolted together by means of allen screws. Neoprene rubber gasket (1mm thick) is used to prevent leakage from all joining surfaces. The chord and the span of the test section are 283 mm and 475 mm respectively. Square cross section (25mm X 25 mm) is used

for the serpentine passage and for the leading edge passage. Trapezoidal cross section is used for trailing edge passage. Ribs and pin-fins are provided as shown in Figure 3 in passages. No film cooling holes are provided in current setup. Dimensional details of test section are shown in Table 2.

The tip of the test section is having detachable tip plates. Tip plate used for current study is described in Table 3 and Figure 3. Diameter of tip holes dA is same for all tip holes except in the serpentine passage where the end hole dB is bigger than dA, as in a real gas turbine blade.

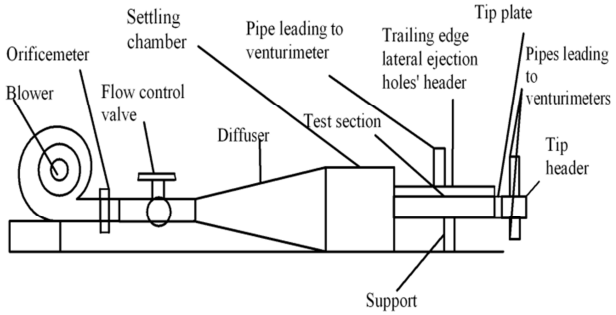

Figure 2: Schematic of the set-up.

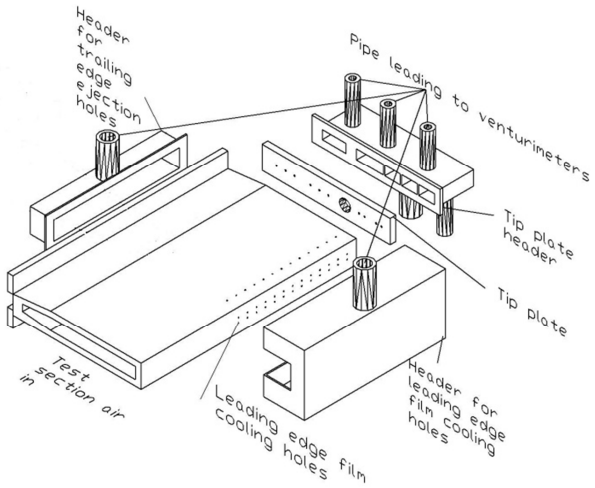

Figure 3: The test section.

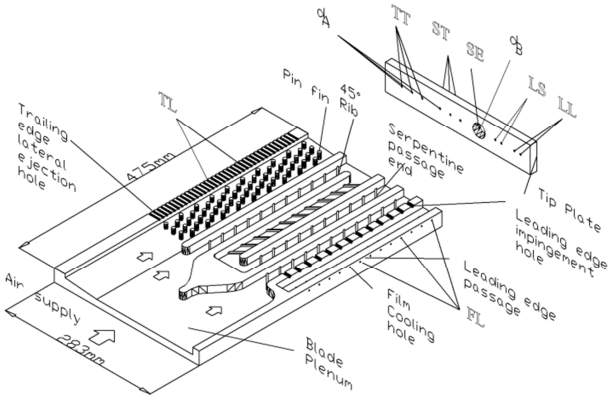

Figure 4: Sectional view of the test section.

Flows from different holes are collected in six different headers. The positions of headers are shown by capital letters. Following six flows are collected,
LL- tip holes of leading most passage of the leading edge passage receiving impinging jet from impingent holes.
LS-tip holes of supply passage of the leading edge passage.
SE-serpentine passage end hole.
ST-serpentine passage tip holes.
TT-trailing edge passage tip holes.
TL- trailing edge passage lateral ejection holes.
FL- film cooling holes of leading edge

3.0 NUMERICAL APPROACH AND PROCEDURE

The computational fluid dynamics code selected to solve this problem is FLUENT version 6.2. Pre-processor of FLUENT called GAMBIT is used for development of the computational geometry and subsequently 3D grid. Figure 5 shows computational domain. Figure 6 through Figure 7 shows computational grid.

3.1 Computational Grid

Computational domain as shown in Figure 5 is consisting of three passages with staggered ribs, pin-fins, tip holes, impingement holes and lateral ejection holes (not labeled). Uniform grid, except in holes is made up of tetrahedral elements. Number of elements in computational domain are 8, 34,008. Wall functions are used to avoid fine grid at the wall.

Table 2: Dimension details of test section

Parameter	Value	Passage
Hydraulic diameter of leading edge passage, mm, [SQUARE]	25	Leading edge passage
Diameter of film cooling holes, mm	2	
Diameter of impingement hole, mm	5	
Number of film cooling holes X row of film holes	13X4	
Spacing of film cooling holes, mm	20	
Spacing of impingement holes, mm	20	

Hydraulic diameter of passage, mm, [SQUARE]	25	Serpentine passage
Angle of ribs to flow direction, deg	45	
Pitch of ribs P, mm	25	
Pitch to height ratio of ribs, P/e	10	
Rib height e, mm	2.5	
Rib height to hydraulic diameter ratio, e/d_h	0.1	
Thickness of divider wall of passage, mm	12.5	
Hydraulic diameter of trailing edge passage, mm, [TRAPEZOIDAL]	27.76	Trailing Edge passage
Diameter of trailing edge ejection holes, mm	3.125	
Diameter of pin in trailing edge passage, mm	6	
Length to diameter ratio for trailing edge ejection holes, mm	7	
Number of trailing edge lateral ejection holes X row of holes	37X1	
Spacing of lateral ejection holes, mm	7.5	
Pitch to diameter ratio of pins	2.5	

Table 3: Dimensional details of tip plates

Tip plate No.	Diameter of tip hole, d_A, mm	Diameter of serpentine passage end hole, d_B, mm	r_d	d_A/d_B
1	4.0	14.0	0.56	0.29

Grid is selected in such way that average y+ for wall bounded cell is greater than 5 (beyond laminar sublayer), since wall function cease to be valid in the viscous layer. Here values of average wall cells y+ existing her are ranging from 12.76 to 16.55. Figure 6 to Figure 7 shows grid used for current computation.

3.2 Turbulence Model

The standard k-ε model is applied. Scheme of discretization for governing equation is finite volume approach. With this approach, the Reynolds-averaged Navier-Stokes equations are solved numerically along with transport equation for the turbulent kinetic energy and dissipation rate. For near wall treatment standard wall functions proposed by Launder and Spalding [8] are used. Flow here is assumed to be steady and incompressible. Properties of the fluid, air is assumed to be constant. Since in this case air is behaving as incompressible, continuity is satisfied using a semi-implicit method for pressure linked equations, called as SIMPLE procedure is employed. Equations are solved implicitly assuming steady flow. Convective scheme used is first order upwind scheme.

3.3 Solution Convergence

Each iteration is done implicitly. The convergence of the computational solution is determined based on scaled residuals for governing equations, and many predicted variables. The total residual for a given variable is based on the imbalance in an equation for conservation of that variable summed over all computational cells. The convergence criterion set for all variables was 10^{-4}. The solution is considered to be converged when all of the scaled residuals are less than or equal to these default settings.

3.4 Computation procedure

Initially problem is solved considering laminar flow for few iterations (70) with different exit pressures as existing in experimental set up are applied. After that flow is treated as turbulent flow and inlet values of k and ε are specified considering 5% turbulence intensity and hydraulic diameter at inlet.

4.0 RESULTS AND DISCUSSION

Here two inlet mass flow rate are considered. Table 4 to Table 6 shows comparison for given case between numerical and experimental values. Percentage difference in predicted and measured supply pressure (%Δp) is evaluated based on measured value. Difference in prediction of major mass flow rates found to be of range 2.59 % to 8.5%. Experimental data is having maximum uncertainty of ±4%, uncertainty is larger in smaller mass flow rate measurements than large mass flow rate measurements. For smaller mass flow rates error in prediction is 0.85% to 20.4% this may be because of larger uncertainty associated. Thus prediction of mass flow rate is reasonably good with these k-ε models. It predicts higher pressure at inlet. Prediction of pressure at inlet is having difference of range 57.0 % to 64 % with respect to experimental data. There is no appreciable change in prediction with variant of k-ε models on mass flow distribution and inlet pressure. RNG k-ε shows better results. Prediction of inlet pressure is poor, as anisotropy in turbulence occurring due to secondary flows existing can't be mapped properly and existing y+ is relatively low (12.76 to 16.55) than recommended (~30).

Figure 8 shows pressure contour for at the symmetry plane. It shows that little passage pressure drop takes place in trailing edge as compared to pressure drop in leading edge passage and ribbed serpentine passage respectively. Figure 9 shows pressure contour in plane perpendicular to y-axis at distance y = 455mm from inlet. In this plane different pressures are observed. Figure 10 shows velocity contours at symmetry. It shows passage highest velocity in serpentine passage. In first and second bends of serpentine passage shows pockets of low velocity at corners. It clearly shows thicker boundary layer at left side and thinner boundary layer at right side on upstream of the bend. Figure 11 shows vector plot for velocity at symmetry plane. It shows interesting feature that at symmetry, velocity vectors are pointing opposite to ribs. This because, inclined ribs forms cross-stream secondary flow. Flow moves along rib near wall, at symmetry it will be in opposite direction as shown in Figure 12. Figure 13 shows velocity vectors in first bend in a plane perpendicular to y axis (limb of serpentine passage) at distance y =455 mm from inlet. This figure clearly shows two vortices at right ride (exit of bend). These two vortices are not symmetrical about camber plane, showing effect of presence of ribs on secondary flows created by bend. Figure 15 shows velocity contour for leading edge passage at symmetry. This figure clearly shows impingement. It also indicates jet deflection is reduced in leading edge passage due to axes film cooling holes in the same plane to that of axis of impingement jet as compared case without film cooling holes.

Table 4: Comparison between numerical and experimental results for $\dot{m}_{tot}$ = 0.02426 kg/s

Exit location	$\%\,\dot{m}_{tot}$ (Expt.)	$\%\,\dot{m}_{tot}$ Stand. k-ε	$\%\,\dot{m}_{tot}$ RNG k-ε	$\%\ \Delta\dot{m}$ Stand. k-ε	$\%\ \Delta\dot{m}$ RNG k-ε	p_{exit}, Pa (boundary condition)
LL	3.51	3.58	3.58	-1.99	-1.99	-377.64
LS	4.49	4.45	4.45	0.89	0.89	-345.27
SE	25.39	26.78	26.45	-5.47	-4.17	-195.18
ST	4.95	5.96	5.94	-20.40	-20	-160.84
TL	35.57	34.65	34.65	2.59	2.59	0
TT	5.97	6.19	6.15	-3.69	-3.02	-126.51
FL	20.12	18.39	18.80	8.59	6.56	-515.96

Table 5: Comparison between numerical and experimental results for $\dot{m}_{tot}$ = 0.01851 kg/s

Exit location	$\%\,\dot{m}_{tot}$ (Expt.)	$\%\,\dot{m}_{tot}$ Stand. k-ε	$\%\,\dot{m}_{tot}$ RNG k-ε	$\%\ \Delta\dot{m}$ Stand. k-ε	$\%\ \Delta\dot{m}$ RNG k-ε	p_{exit}, Pa (boundary condition)
LL	3.55	3.58	3.58	-0.85	-0.85	-225.63
LS	4.53	4.45	4.45	1.77	1.77	-211.9
SE	25.23	26.87	26.53	-6.50	-5.15	-117.72
ST	5.00	5.95	5.94	-19	-18.8	-89.27
TL	35.60	34.54	34.56	2.98	2.92	0
TT	5.91	6.16	6.13	-4.23	-3.72	-66.71
FL	20.18	18.44	18.80	8.62	6.84	-317.85

Table 6: Comparison between numerical and experimental inlet pressures

Inlet mass flow rate	p_{in}, Pa Expt.	p_{in}, Pa Stand	p_{in}, Pa RNG.	% Δp Stand. k-ε	% Δp RNG k-ε
0.02426	1037.94	1697.56	1631.18	-63.55	-57.16
0.01851	602.33	995	956.4	-65.19	-58.78

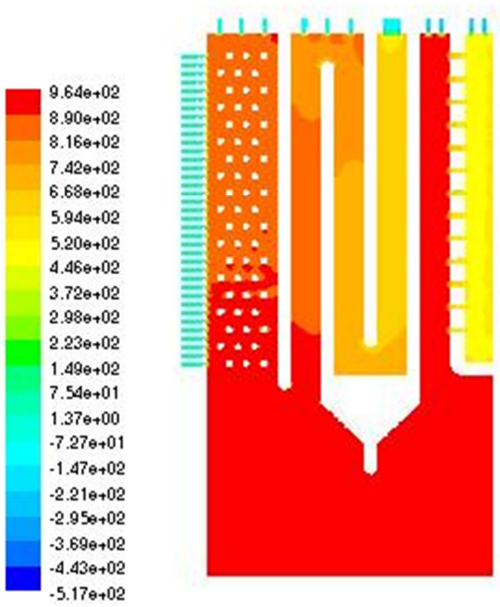

Figure 8: Static pressure contours at symmetry plane

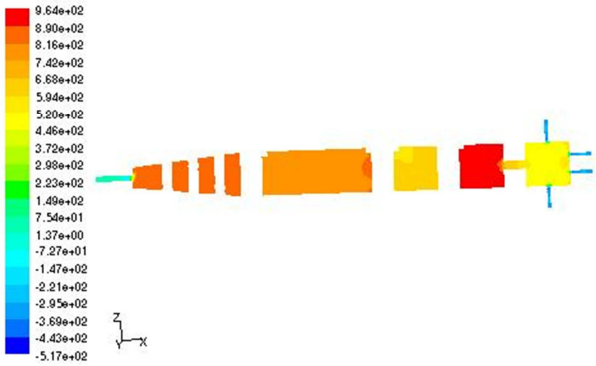

Figure 9: Static pressure contour in plane perpendicular to y axis at y=455mm from inlet.

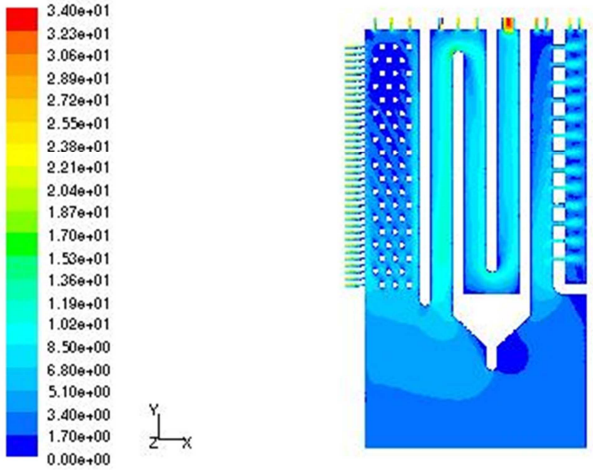

Figure 10: Velocity contours at symmetry plane.

Figure 11: Vector plot at symmetry plane.

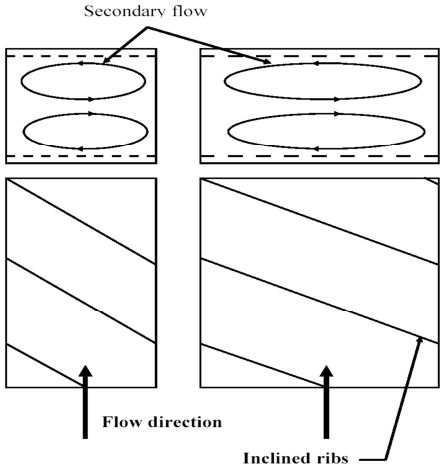

Fig. 12: Secondary flows in ribbed passage [1]

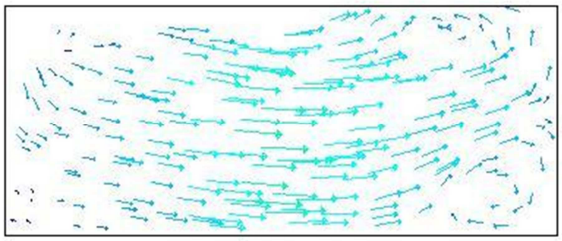

Figure 13: Vector plot in first bend in a plane perpendicular to limb of serpentine at distance of 455mm from the inlet.

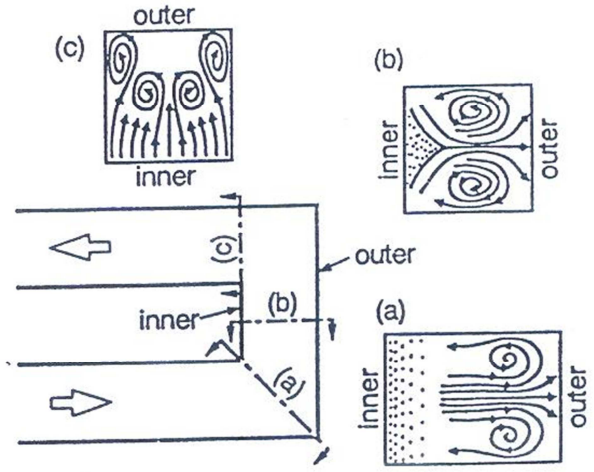

Figure 14: Bend induced secondary flows with smooth passage [9]

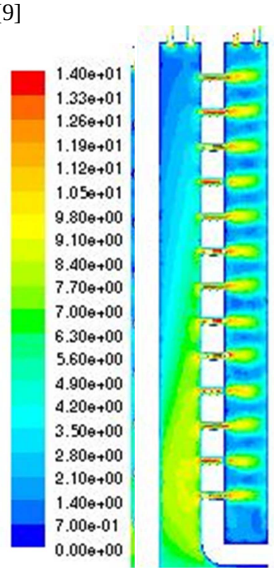

Figure 15: Velocity contours at symmetry plane in leading edge passage.

Figure 2: Stern hull designs for podded propulsion system.

5.0 CONCLUSION

It shows capability of k-ε models with standard wall function to predict flow distribution. It shows good agreement for mass flow prediction. The supply pressure prediction is poor. There is no appreciable change in prediction with Standard and RNG variant of k-ε models on mass flow distribution. RNG k-ε gives closer agreement of supply pressure to experimental data. Secondary flows existing due to inclined ribs and due to bend are observed. Secondary flows due to bends are affected by presence of ribs.

In future prediction with low Reynolds number version of k-ε and RSM (Reynolds Stresses Modeling) can be done to improve pressure prediction.

ACKNOWLEDGEMENTS

Author is grateful to Prof. A. W. Date and Prof. R. P. Vedula, Department of Mechanical Engineering, IIT Bombay, for useful discussion. The staffs of Central Workshop and Steam Power Lab., IIT Bombay, are acknowledged for their help in fabrication of the experimental setup.

REFERENCE

1. Han, J. C., Dutta, Sandip and Ekkad Srinath. (2000). *Gas Turbine Heat Transfer and Cooling Technology*, Taylor & Francis Inc. London, 1st Edition, pp 2-25.
2. Borse, S. L. and Date, A. W., (2006). *Flow Distribution inside Internally Cooled Gas Turbine Blade without Film Cooling Holes, 18th National & 7th ISHMT- ASME Heat and Mass Transfer Conference*, IIT Guwahati, India, paper no-G075, .January 4-6.
3. Borse, S. L. and Date, A. W., (2006) *Flow Distribution inside Internally Cooled Gas Turbine Blade with Film Cooling Holes, 13th International Heat Transfer Conference*, Sydney, Australia.
4. Borse, Sachin L., (2006) *Numerical Study of Flow Distribution inside Cooled Non-Rotating Gas Turbine Blade without Pin Fins, Ribs and Film Cooling Holes, 33rd National and 3rd International Conference on Fluid Mechanics and Fluid Power*, IIT Bombay, India, paper no-1301, Dec 7-9.
5. [5]Borse, Sachin L., (2006). *Numerical Study of Flow Distribution inside Cooled Non-Rotating Gas Turbine Blade with Pin-Fins and without Ribs and Film Cooling Holes, National Conference on Advances in Heat Transfer and Fluid Dynamics*, A. M. University, Aligarh, India, paper no. SHTF-04, September 16-17.
6. Borse, S. L., (2006) *Prediction of Flow Distribution in Non-Rotating Cooled Gas Turbine Blade with Pin-Fins and Ribs and without Film Cooling Holes, 33rd National and 3rd International Conference on Fluid Mechanics and Fluid Power*, IIT Bombay, India, paper no. 1726, December 7-9.
7. Hwang, G. J., Tzeng, S. C., Mao, C. P. and Soong C. Y., (2001). *Heat Transfer in a Radially Rotating Four-Pass Serpentine Channel with Staggered Half- V Rib Turbulators*, J. Heat Transfer, vol. 123, pp. 39-50.
8. Launder, B. E. and Spalding, D. B.,(1974) *The Numerical*

Computation of Turbulent Flows, Computer Methods in Applied Mechanics and Engineering, vol-3, pp. 269-289.

9. Mochizuki S., Murata A., Fukunaga M.,(1997). *Effects of Rib Arrangement on Pressure Drop and Heat Transfer in Rib Roughened Channel with A Sharp 180 Deg. Turn*", ASME Journal of Turbomachinery, vol- 119, pp. 610-616,